The Effects of Simulated Airway Diseases and Affected Flow Distributions on Aerosol Deposition

Gabriela Apiou-Sbirlea PhD, Ira M Katz PhD, and Ted B Martonen PhD

BACKGROUND: Experimental and theoretical aspects of targeted drug delivery have been addressed several times in this journal. Herein, a computational study of particle deposition patterns within healthy and diseased lungs has been performed, using a validated aerosol dosimetry model and a flow-resistance model. OBJECTIVE: To evaluate to what extent the uneven flow distributions produced by the physical manifestations of respiratory diseases affect the deposition patterns of inhaled aerosolized drugs. METHODS: Diseases were simulated by constrictions and blockages, which caused uneven flow distributions. Respiratory conditions of sedentary and pronounced activities, and of particle sizes ranging from 0.1 μm to 10 μm, were used as the basis for the calculated deposition patterns. RESULTS: Findings are presented that describe flow as a function of airway disease state (eg, flow redistribution). Data on the effects of lung morphologies, healthy and diseased, on compartmental (tracheobronchial and pulmonary) and local (airway generation) aerosol deposition are also given. By formulating these related factors, modeling results show that aerosolized drugs can be effectively targeted to appropriate sites within lungs to elicit positive therapeutic effects. CONCLUSIONS: We have addressed the complexities involved when taking into account interactive effects between diseased airway morphologies and redistributed air flows on the transport and deposition of inhaled particles. Our results demonstrate that respiratory diseases may influence the deposition of inhaled drugs used in their treatment in a systematic and predictable manner. We submit this work as a first step in establishing the use of mathematical modeling techniques as a sound scientific basis to relate airway diseases and aerosolized drug delivery protocols. *Key words: airway disease; flow redistribution; aerosol deposition; mathematical model.*
[Respir Care 2010;55(6):707–718.

Introduction

Clinical studies suggest that the targeting of inhaled pharmaceuticals to specific sites within lungs may enhance their efficacies.[1-6] Variables that influence the spatial distributions of deposited particles include aerosol characteristics, ventilatory parameters, and lung morphologies. Considering the latter, even differences in lung morphologies among healthy subjects under controlled laboratory conditions present difficulties in interpreting inhalation exposure data (ie, inter-subject variability). These uncertainties in deposition increase when subjects suffer from an airway disease.[7,8] The restriction of airway caliber, and perhaps complete blockage, can be the result of many lung pathologies. For example, asthma can produce a reduction in airway lumen due to either bronchoconstriction or inflammation. Zeidler et al[9] reported an inhomogeneous pattern

Gabriela Apiou-Sbirlea PhD and Ira M Katz PhD are affiliated with Air Liquide, Research and Development, Claude-Delorme Research Center, Jouy-en-Josas, France. Gabriela Apiou-Sbirlea PhD is also affiliated with the Biomedical Research Institute Mondor, (INSERM, UMR 955), University Paris Est Créteil, Créteil, France. Ira M Katz PhD is also affiliated with the Department of Mechanical Engineering, Lafayette College, Easton, Pennsylvania. Ted B Martonen PhD is affiliated with CyberMedicine, Laguna Beach, California, and with the Department of Medicine, University of North Carolina, Chapel Hill, North Carolina.

The authors have disclosed no conflicts of interest.

Correspondence: Gabriela Apiou-Sbirlea PhD, Biomedical Research Institute Mondor (Institut National de la Santé et de la Recherche Médicale (INSERM), Unité Mixte de Recherche (UMR) 955), Department of Cell and Respiratory Biomechanics, School of Medicine, 3rd floor, office 3060, 8 Rue du Général Sarrail Créteil 94010 France. E-mail: gabriela.apiou@inserm.fr.

of small airway abnormalities in asthmatic patients observed via high-resolution computed tomography. In a different pathology, cystic fibrosis can produce a complete blockage, or occlusion, due to a mucus plug.[10] While there have been mathematical modeling studies of the uneven flow distributions due to the non-symmetric nature of the lung,[11,12] they have not addressed the effects due to airway obstructions.

Thus, a question plaguing clinicians has been this: to what extent do the uneven flow distributions produced by the physical manifestations of respiratory diseases affect the deposition patterns of inhaled aerosolized drugs? For example, would a narrowing of the lumen increase or decrease the deposition in an airway? In some cases the flow and aerosol mass are diverted (or shunted) to other pathways; therefore, decreasing deposition in the affected segment. However, increased deposition may be observed within the narrowed airways due to an increase in the efficiency of the inertial impaction mechanism; that is, a reduced airway diameter will result in an increased velocity and therefore increased deposition if mass flow through it is preserved. It must also be remembered that the deposition mechanisms of sedimentation and diffusion are inversely related to flow velocity. Therefore, how deposition is affected depends on the specific values of particle sizes, airstream velocities, and airway dimensions. Moreover, the enhanced deposition observed clinically may likely be attributed to the interception deposition mechanism at an obstruction.

To study these complex interrelations we have integrated 2 mathematical models and related computer codes. First of all, a flow-resistance model based on the work of Pedley et al[13] was used to determine the uneven flow distributions that may be ascribed to airway constrictions.

Second, based on the resulting airstreams, aerosol deposition patterns were determined using the computer model developed by Martonen et al.[14] The latter dosimetry model has been validated by comparisons of calculated deposition patterns with data obtained via inhalation exposures using volunteer human subjects[14-16] and patients suffering from chronic obstructive pulmonary disease[17] and asthma.[18]

Methods

Aerosol Dosimetry Model

The validated aerosol deposition model used in this work is based on the straightforward premise that the physical and biological processes governing the transport and deposition of airborne drugs can be simulated if lung morphologies, aerosol characteristics, and ventilatory parameters are known (ie, available). Since its creation[15] the model has evolved to become evermore anatomically realistic[19] with clinical applications in mind.[20] Hence, in its development a great deal of emphasis has been placed on testing it via comparisons of theoretical predictions with data from human inhalation experiments (as cited above). The prominent mechanisms of particle deposition in lung airways are inertial impaction, sedimentation, and diffusion.[21] The simulations yield deposition fractions within each airway generation that are normalized to the total amount of aerosol entering the lungs. The morphology developed by Soong et al[22] is used to describe normal adult human lungs in this study. It is a symmetric, dichotomously branching network of cylindrical tubes. The tracheobronchial compartment consists of 17 generations of conducting airways numbered from 0 (trachea) through 16 (terminal bronchioles) and the pulmonary compartment consists of 7 generations of alveolated airways numbered from 17 (respiratory bronchioles) through 23 (alveolar sacs). Each generation consists of 2^I identical airways, where I is the generation number. This model is based on the work of Weibel[23] but is designed to account for intersubject variability. The successful employment of the aerosol dosimetry model in the clinical arena has been documented in this journal by Martonen and colleagues.[16,20]

Although particle deposition mechanisms are relatively well understood and have been explicitly formulated,[21] it should be recognized that the processes are inherently rather complicated events involving interactions among variables. Let us consider a simple example involving an airway dimension, namely the tube diameter d. Obviously, it is indicative of the distance to an airway's wall that a particle must travel to be deposited. But the mean velocity of an airstream transporting a particle, U, is inversely related to an airway's cross-sectional area. That is, $U \propto 1/d^2$. Hence, a decrease in the value of d will have mutually competing effects. It will decrease the distance per se to the collection surface, but will increase the transit velocity through the airway. In other words, the residence time in an airway $\Delta t = L/U$ will be decreased, thereby allowing less time for deposition to occur. The above has been a single straightforward example, and many such interactions affect the deposition efficiencies of the inertial impaction, sedimentation, and diffusion mechanisms. We refer the interested reader to the work of Isaacs et al[21] for details.

Flow-Resistance Model

Flow distribution through airways is driven by a pressure drop, Δp(=dyne/cm^2), that overcomes resistance to motion. Mathematically, this is simply

$$\Delta p = QR \quad (1)$$

where Q is the volumetric flow rate, and R is the flow resistance. The flow resistance, R (dyne $\times$ s/cm^5), of an individual airway is[13]

$$R = \frac{13.3\mu L}{d^4}\left(Re\,\frac{d}{L}\right)^{1/2} \quad (2)$$

where μ is the absolute viscosity, L is the length of the airway, d is the diameter of the airway, and Re is the flow Reynolds number. The dimensionless Re is given by

$$Re = \frac{\rho U d}{\mu} \quad (3)$$

where U is the average velocity and ρ is the fluid density.

Solutions to this air flow model for a healthy morphology follow 2 approaches, depending on whether or not Q entering the lungs is known. If it is, R may be calculated for each generation directly using Equation 2 with the proper morphology data from Soong et al.[22] In turn, R is used to determine Δp using Equation 1. Within airway networks, low resistances may be combined based on electrical resistance analogs for series circuits (along a designated branch) and parallel circuits (between airways of the same generation in different branches). Alternatively, if Q is unknown, an iterative procedure may be used, assuming Δp is known. For example, Q is assumed, thus allowing for the calculation of R, and therefore, Δp. The resulting Δp is then compared to its known value and Q is adjusted accordingly until it converges to the known value.

Deposition Simulations

Aerosol deposition computations were performed using biologically realistic 3-dimensional airway morphologies.[19,20] However, to illustrate the effects of an uneven flow distribution caused by the physical manifestation of an airway disease, we employed the stylistic airway system shown in Figure 1. It is submitted to RESPIRATORY CARE as a first step in modeling air flow maldistribution. As an example, let us consider that the reduction in airway lumen occurs in one of the 4 branches of generation I = 2. The reduction per se may be partial when corresponding to the bronchoconstriction or inflammation of asthma,[18] or total when corresponding to occlusion by a mucus plug with cystic fibrosis.[10] Thus, there are 3 flows to be considered, through the diseased airway, through the branch adjacent to it, and through the 2 free branches (which will be equal). The specific model herein has the obstruction at I = 2; but, it should be understood that, due to the branching structure of the lung, it is qualitatively representative of an obstruction at any generation located more distal. Asthma and cystic fibrosis are 2 examples we choose to illustrate how diseases manifest in airways obstructions and/or occlusions and how the induced effects are represented into a mathematical formulation. However, the same methodology can be applied for all airways narrowing based pathologies (eg, bronchogenic carcinoma, foreign body, lung resection).

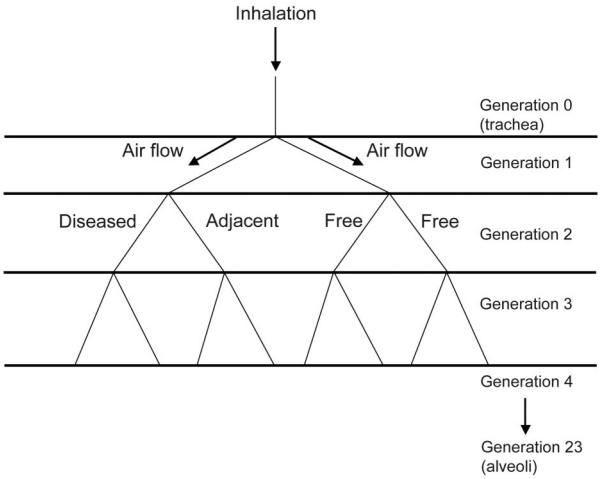

Fig. 1. An idealized airway network and related nomenclature. This simplistic morphology is presented for demonstration purposes only to show how disease, flow, and resistance are associated. Computer generated anatomically realistic 3-dimensional lung morphologies used in this work have been developed by Martonen et al and published in this journal.[20]

The aerosols simulated in the study will be monodisperse, with geometric diameters ranging from 0.1 μm to 10.0 μm. Their material density will be 1.0 g/cm^3. These sizes are typical of the constituents of polydisperse aerosols produced in clinical laboratories by nebulizers, metered-dose inhalers and dry-powder inhalers.

To demonstrate the importance of breathing conditions on particle deposition, we shall consider 2 enveloping scenarios. The ventilatory parameters will correspond to sedentary (tidal volume 500 mL, frequency 14 breaths/min, inspiratory flow 14 L/min) and pronounced (tidal volume 2,449 mL, frequency 24.5 breaths/min, inspiratory flow 120 L/min) respiratory activities.

Results

Flow Distribution

Consider the lung model depicted in Figure 1. For a healthy subject each of the 4 branches in generation I = 2 will have the same diameter. During pronounced respiratory activity the inspiratory flow rate through each of the 4 branches will be the same and be equal to 30 (120/4) L/min. To simulate disease, the diameter of the affected airway will be reduced. A diameter ratio of

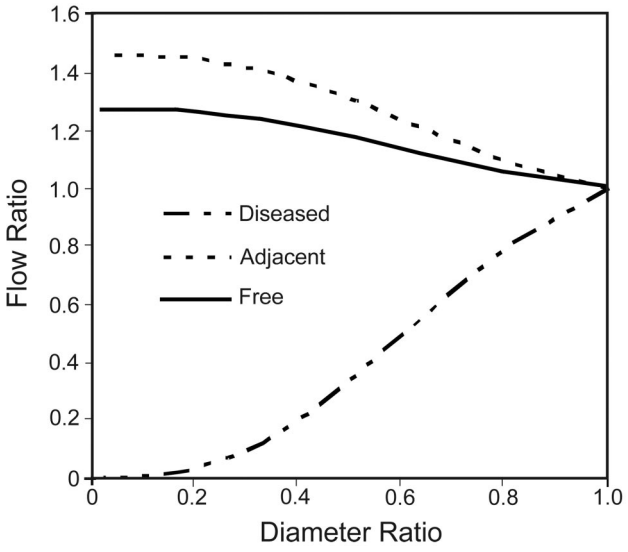

Fig. 2. The effect of airway disease (in terms of the diameter ratio) on flow redistribution for pronounced respiratory activity.

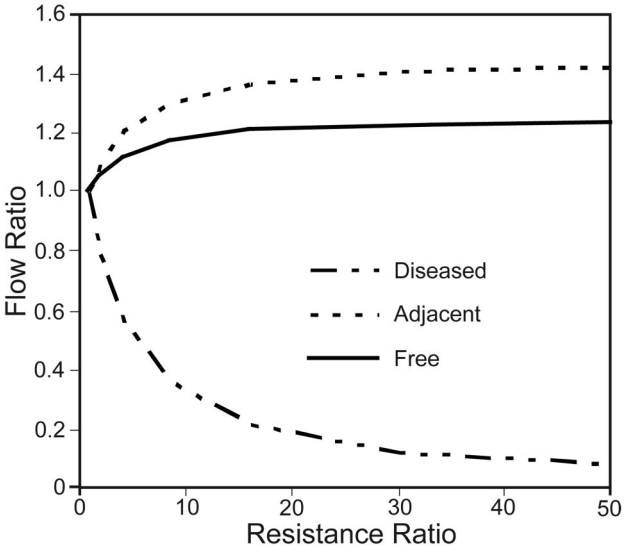

Fig. 3. The effect of airway disease (in terms of the resistance ratio) on flow redistribution for pronounced respiratory activity.

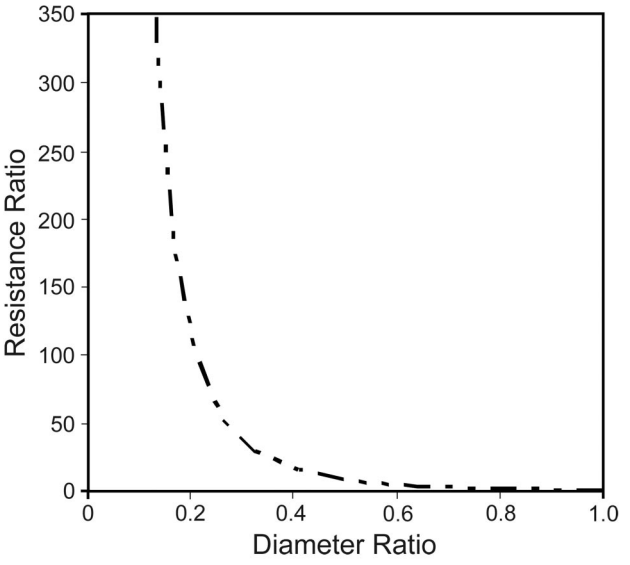

Fig. 4. The relationship between the diameter ratio and resistance ratio parameters for the diseased airway and pronounced respiratory activity.

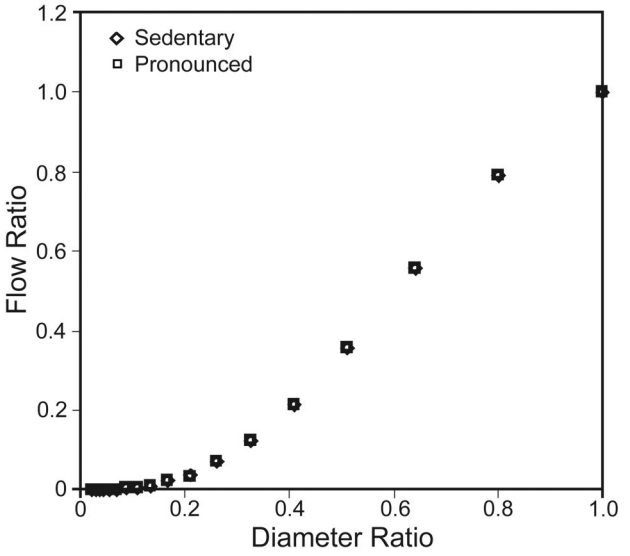

Fig. 5. Comparison of the effect of airway disease between sedentary and pronounced respiratory activities.

disease-to-healthy states will reflect the amount that it is constricted. Thus, a diameter ratio of 1 is a healthy state, and 0 is a complete blockage (or occlusion). The flow ratio reflects the change in flow rate compared to the healthy (control) state. Thus, if a constriction reduces the flow through a diseased airway from 30 L/min to 10 L/min the flow ratio will be 0.33 (10/30). However, as the flow rate in the adjacent non-diseased airway increases to 40 L/min, its flow ratio will be 1.33 (40/30).

With this new terminology in mind, let us consider Figure 2, where the results of a flow analysis for pronounced respiratory activity are presented (ie, the flow ratio is plotted as a function of the diameter ratio of the diseased airway). The total flow rate through the trachea is maintained at 120 L/min. On the right-hand-side of the plot the 3 curves meet at a diameter ratio of 1 and a flow ratio of 1. This is the healthy (control) state, where the flow rates through all 4 branches of generation 2 are the same. Moving to the left along the abscissa, the constriction increases in severity. For a diameter ratio of 0, the flow ratio of the diseased (or blocked) airway is 0. Because the total flow rate through the system is constant (ie, in engineering terms, mass conservation

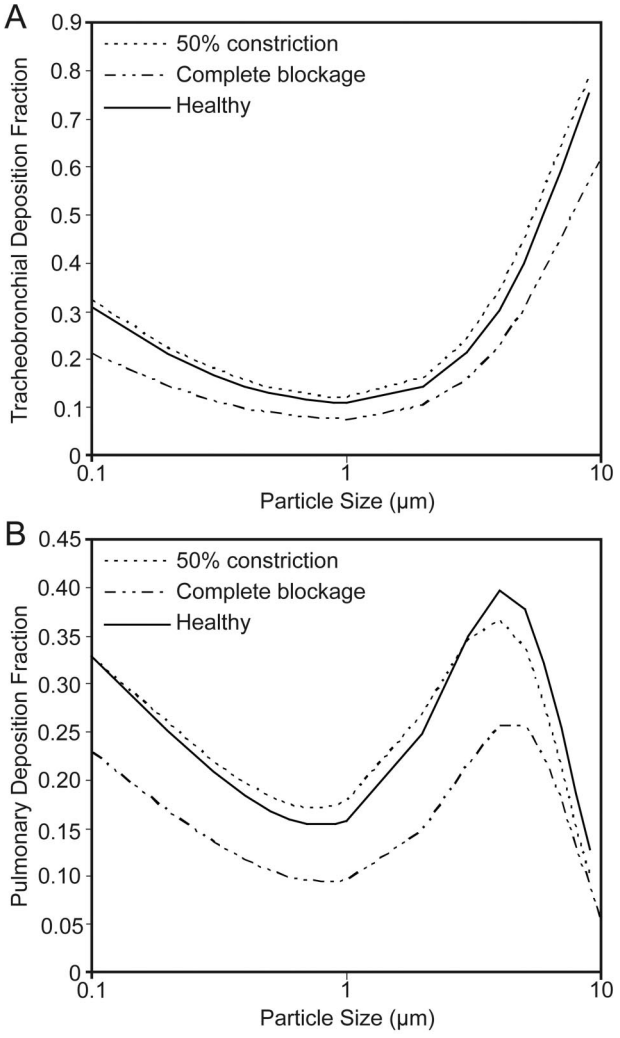

Fig. 6. Effects of lung morphologies, healthy and diseased, on aerosol deposition in the tracheobronchial (panel A) and pulmonary (panel B) compartments for sedentary respiratory activity.

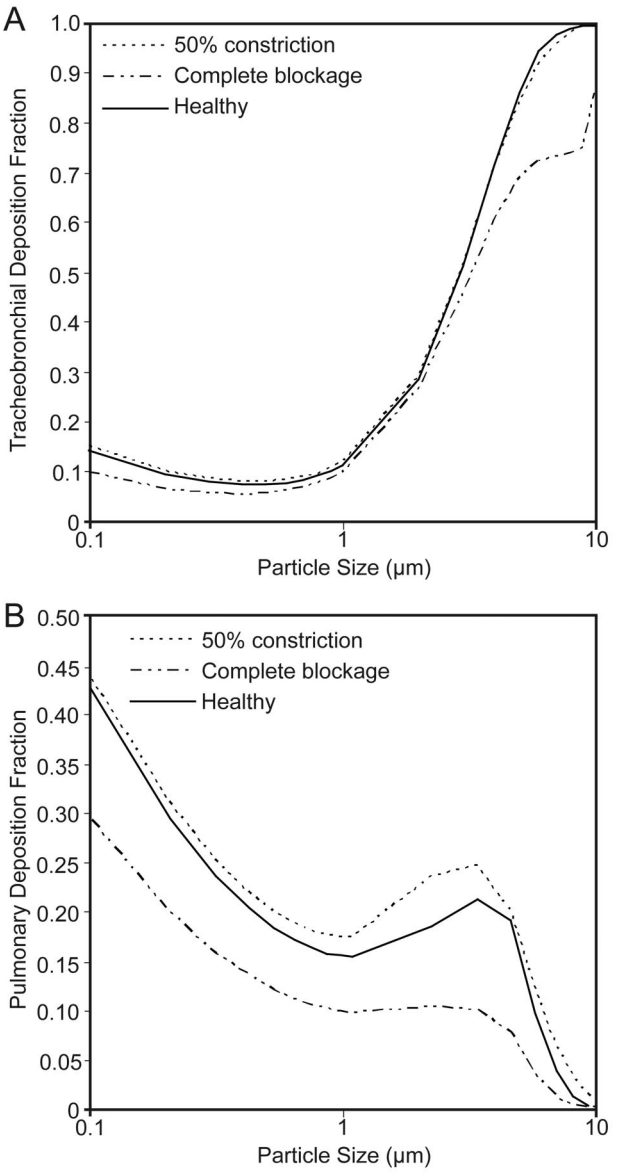

Fig. 7. Effects of lung morphologies, healthy and diseased, on aerosol deposition in the tracheobronchial (panel A) and pulmonary (panel B) compartments for pronounced respiratory activity.

exists), the flow rates through the airway adjacent to the blockage and the identified free airways increase, respectively.

Another way to observe the complex, yet systematic relationship between flow, resistance, and pathology is shown in Figure 3, where the flow ratio is plotted as a function of the resistance ratio of the diseased airway. The relationship between the diameter ratio and the resistance ratio for the diseased airway at the pronounced respiratory activity is shown in Figure 4.

The relationships between flow through the diseased, adjacent, and free branches discussed above for the pronounced respiratory activity can be regarded as a general result because of the computational technique describing flow, which is based on conservation of mass within the airway system. For reference, Figure 5 shows the superimposed curves of the flow ratio as a function of diameter ratio for the diseased airway for pronounced and sedentary breathing conditions.

Aerosol Deposition

An extensive series of computations were performed to illustrate the inter-related effects of lung morphologies (healthy and altered due to disease), ventilatory parameters, and inhaled particle sizes on aerosol deposition patterns. The deposition model was applied to each branch (diseased, adjacent, and free) individually, at its appropri-

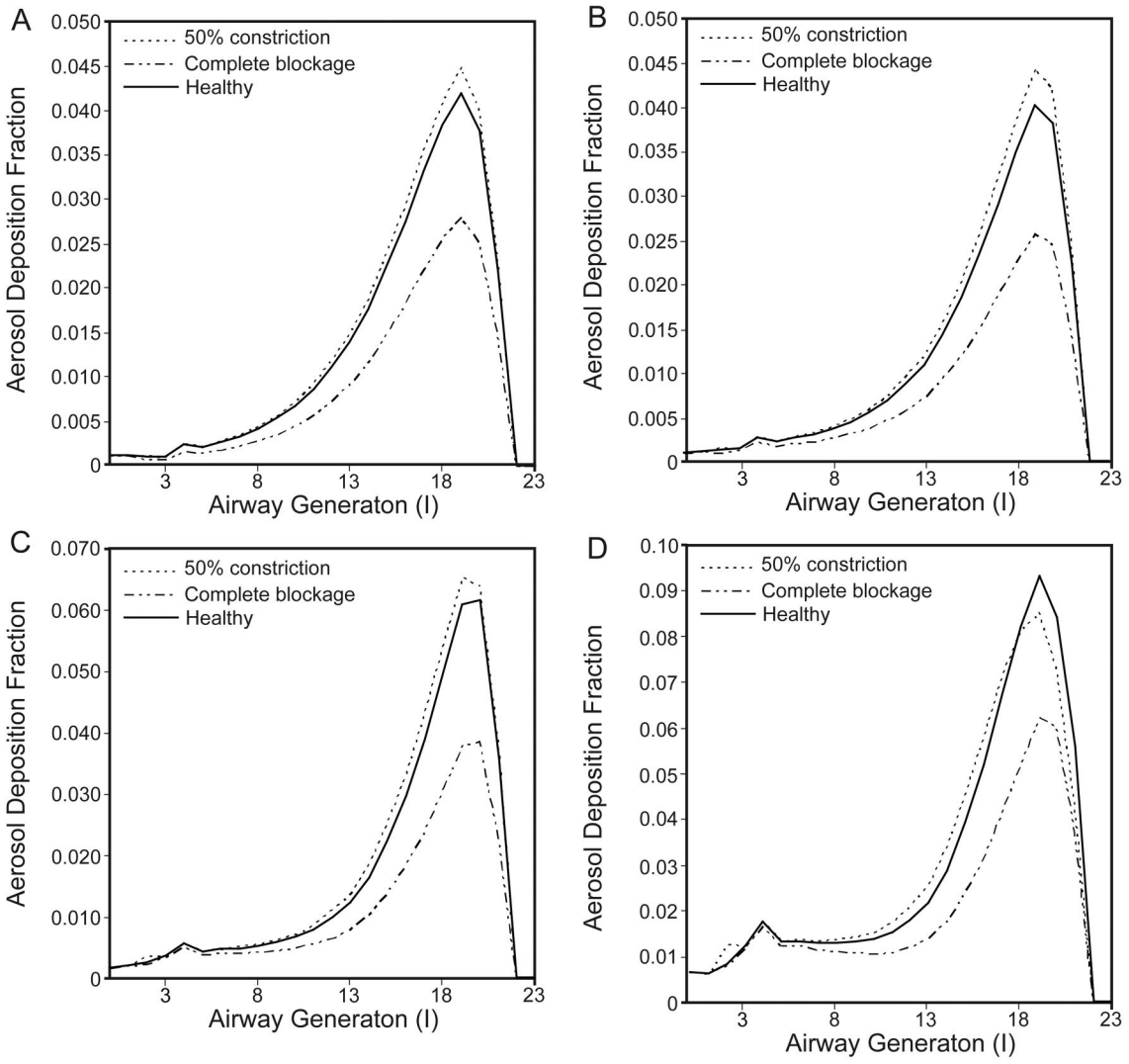

Fig. 8. Monodisperse aerosol deposition patterns within lungs for sedentary respiratory activity. Deposition curves are presented for 2 disease states and a normal (control) case. Particle sizes are 0.5 μm (panel A), 1.0 μm (panel B), 2.0 μm (panel C), and 4.0 μm (panel D) diameter.

ate flow rate. In other words, particle transport was analyzed in all composite airways within each branch, originating at one of the 4 designated sites in generation I = 2 (see Fig. 1) and terminating at the alveoli (I = 23). The resulting branch deposition fractions were then summed to determine total deposition fractions within the lungs.

Figure 6 shows deposition fractions for a wide diameter range of monodisperse aerosols in healthy subjects (controls), patients with a reduced lumen corresponding to a 50% diameter change (diameter ratio = 0.5), and patients with a complete blockage (diameter ratio = 0). Disease is assumed to be located in the single airway within generation I = 2 identified in Figure 1. A sedentary respiratory activity is simulated. Panels A and B give compartmental tracheobronchial and pulmonary deposition fractions, respectively. Figure 7 presents deposition data for pronounced respiratory activity. There is relatively little change in tracheobronchial deposition, except for large particles and severe disease (a complete blockage) as shown in Panel A. Panel B reflects the substantive deposition of large particles in the upstream tracheobronchial compartment. Figure 8 shows aerosol distributions within lungs for a sedentary respiratory activity and a designated range of particle diameters. The generation-by-generation deposition data are presented for 3 lung morphologies: healthy (control), 50% reduction in airway lumen, and complete blockage. Figure 9 shows analogous results for pronounced respiratory activity. In a systematic series of Figures 10–13, generation-by-generation aerosol distributions along the 3 types of branch morphologies considered in this work, namely, the designated diseased, adjacent, and free constituent pathways of the lungs, are displayed. Figure 10

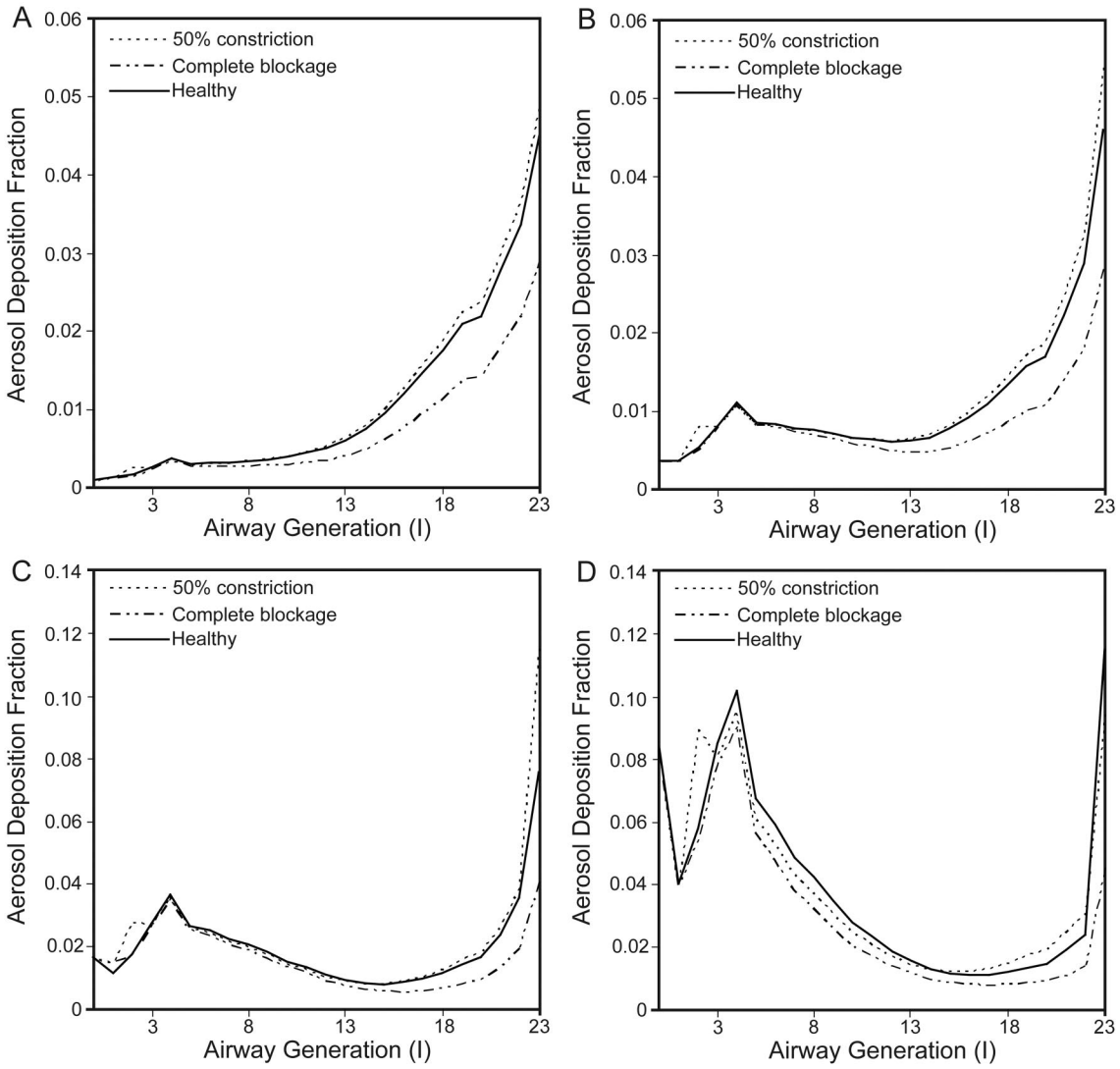

Fig. 9. Monodisperse aerosol deposition patterns within lungs for pronounced respiratory activity. Deposition curves are presented for 2 disease states and a normal (control) case. Particle sizes are 0.5 (panel A), 1.0 μm (panel B), 2.0 μm (panel C), and 4.0 μm (panel D) diameter.

shows results for the constricted (partially blocked) airway and sedentary respiratory activity. For the smaller (0.5 μm and 1.0 μm) particles there is a significant increase in deposition throughout the diseased branch, compared to the non-diseased branches, which is particularly evident in the pulmonary compartment (see Fig. 10A and 10B). For the larger 2-μm particles (see Fig. 10C) there is somewhat less deposition in the upper airways in the constricted branch, except at the site of disease itself. For the largest 4-μm particles the deposition pattern is more complicated because the enhancement occurs in upstream regions and, therefore, fewer particles are available for deposition in the alveolated airways (see Fig. 10D). The effects of an elevated respiratory activity on aerosol delivery are addressed in Figure 11. The panels may be directly compared to their counterparts in Figure 10 to observe the influence of breathing parameters on particle deposition. Clearly, the respective panels differ qualitatively (ie, in shape) and quantitatively (ie, in magnitude), showing that for prescribed particle sizes produced by aerosol delivery devices (eg, metered-dose inhalers) the manners in which patients breath have major effects on the deposition patterns of inhaled drugs.

Of course, there will be no deposition in the distal airways of a severely diseased branch having a complete blockage in generation I = 2. But the question remains: how will this blockage affect deposition in the other branches labeled adjacent and free in Figure 1? Figures 12 and 13 show the results of our simulations for sedentary and pronounced respiratory activities, respectively.

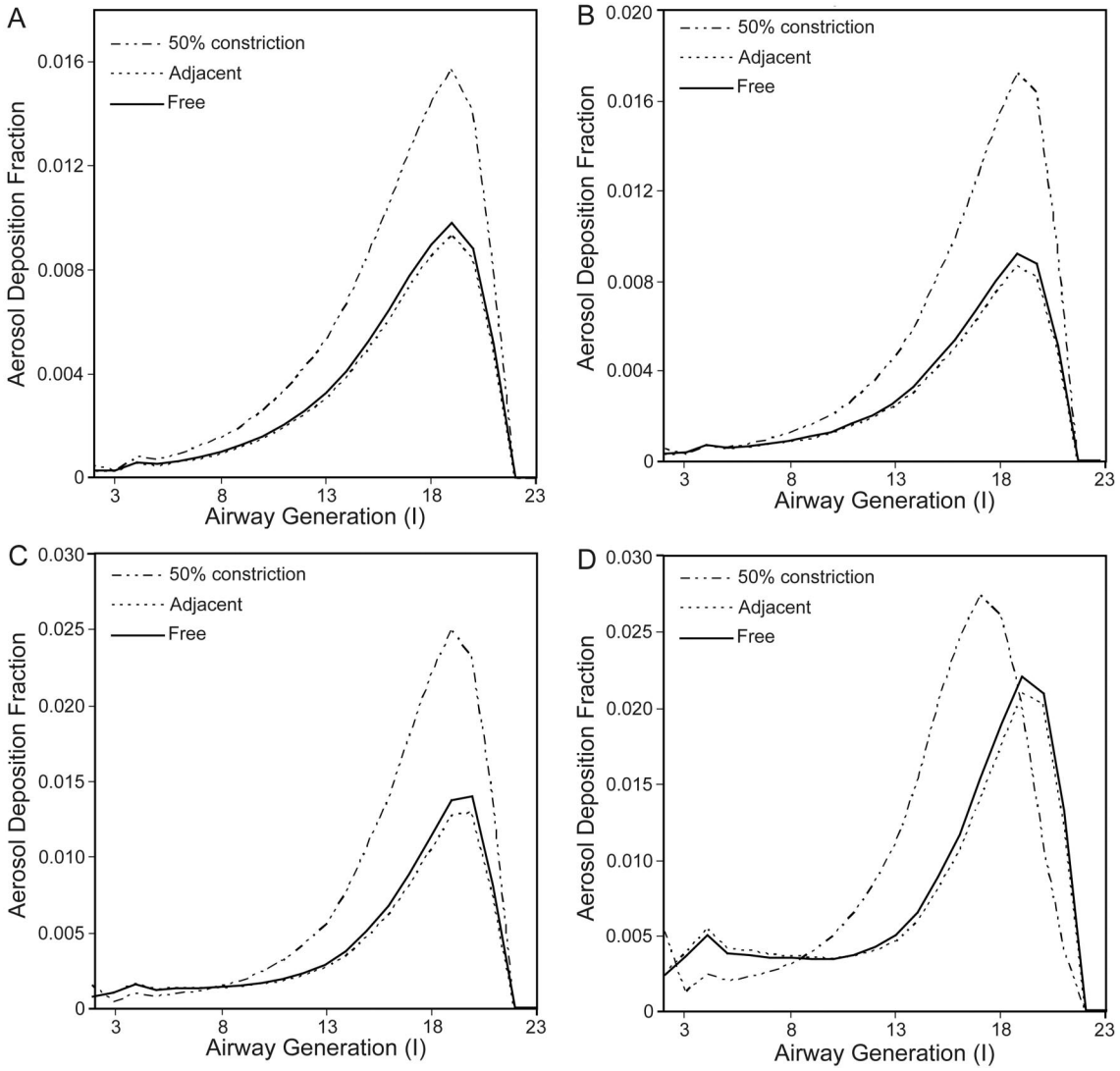

Fig. 10. Aerosol deposition patterns for sedentary respiratory activity along identified branch morphologies. The disease corresponds to a 50% constriction (reduction in diameter ratio). Particle sizes are 0.5 μm (panel A), 1.0 μm (panel B), 2.0 μm (panel C), and 4.0 μm (panel D) diameter.

Discussion

The first step of our approach was the definition of the morphology to be used. That is, one healthy (control) and 2 diseased cases (50% lumen reduction and complete occlusion of one airway on the second generation of the branching network) were considered. The partial constriction could simulate conditions within a patient suffering from asthma, where airway calibers are reduced by bronchoconstriction or inflammation. Computer representations of these pathological conditions are depicted elsewhere. The complete blockage may be representative of cystic fibrosis, where airways are closed by mucus plugs.[10]

The second step consisted in simulating the air flow through the lungs (ie, from trachea down to alveoli). The influence of diameter and resistance ratios, as well as breathing regimes, on the flow rate were analyzed.

Figure 2 shows that the total resistance to flow through the network increases with the severity of respiratory disease, as manifested by the degree of physical airway constriction; hence, a human being must breathe harder with a correspondingly greater Δp to maintain the designated total flow rate. Even the resistances of the identified adjacent and free airways will increase because resistance is a function of flow parameters (see Equation 2).

Figure 3 demonstrates that an order-of-magnitude increase in the resistance (resistance ratio equal to 10) results in an approximately 70% reduction in flow (flow ratio equal to 0.3) through the diseased (constricted) airway.

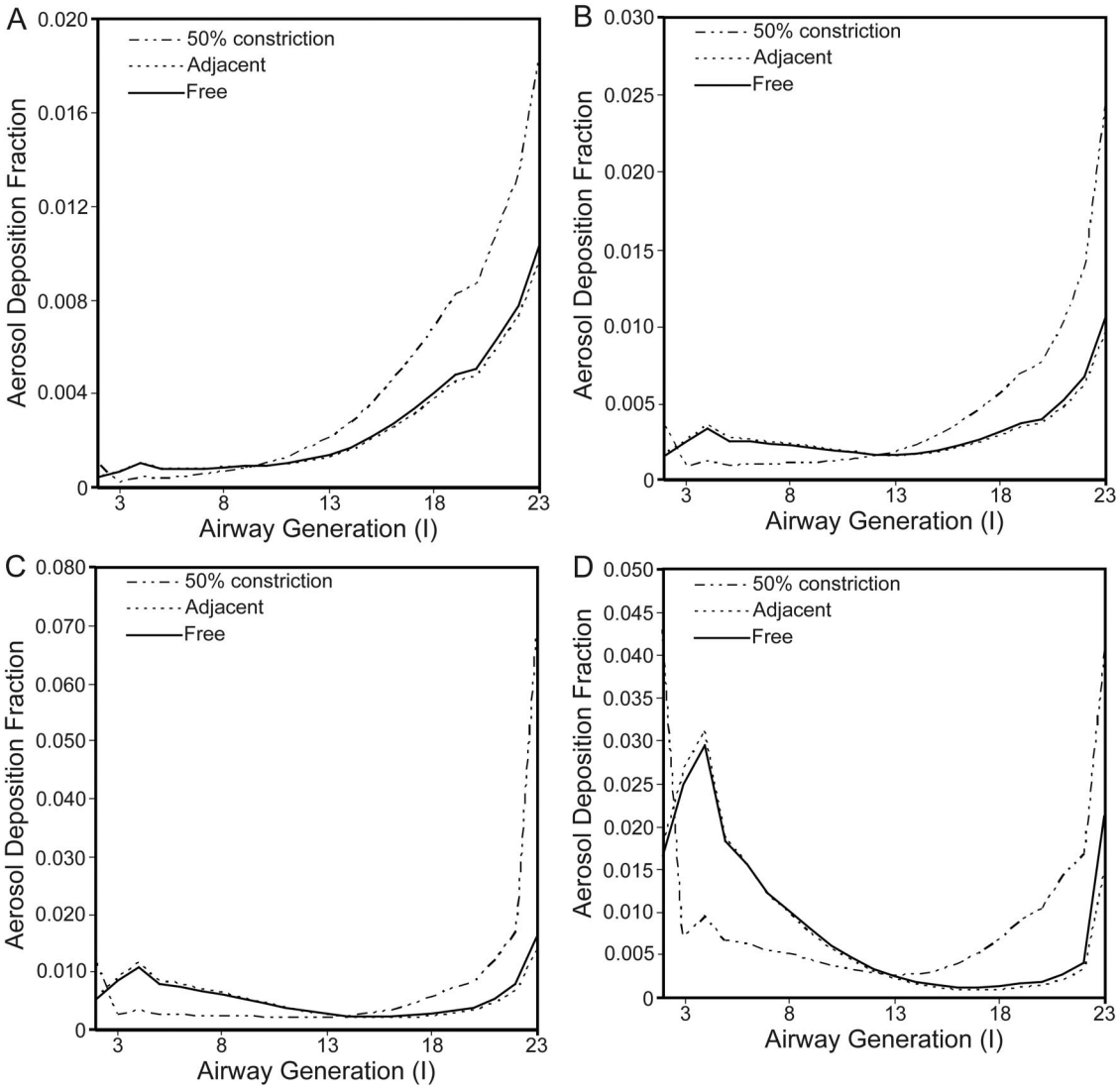

Fig. 11. Aerosol deposition patterns for pronounced activity along identified branch morphologies. The disease corresponds to a 50% constriction (reduction in diameter ratio). Particle sizes are 0.5 μm (panel A), 1.0 μm (panel B), 2.0 μm (panel C), and 4.0 μm (panel D) diameter.

The third step of our approach consisted in performing aerosol deposition computations. They were conducted in an orderly manner to consider inter-subject variability in the medical arena. Figures 6, 8, 10, and 12 address human beings at rest; that is, the healthy volunteer subjects (controls) and patients had sedentary activity ventilatory parameters in the simulated drug delivery protocols. In Figures 7, 9, 11, and 13 pronounced activity ventilatory parameters were used. As noted in the Methods section, the 2 breathing conditions are intended to serve as enveloping scenarios.

For sedentary breathing conditions, partial blockage within the respective diseased branches has a negligible effect on compartmental deposition values. Complete blockage, however, does result in as much as a 50% reduction in both tracheobronchial and pulmonary deposition fractions (see Fig. 6).

For the pronounced ventilator regime there is some increase in pulmonary deposition for the case of partial airway constriction, but a great decrease for the case of complete blockage, over the whole aerosol size range (see Fig. 7).

The deposition data depicted in Figures 8 and 9 indicate that, across the wide ranges of respiratory activities and particle diameters considered, there are relatively negligible effects that may be ascribed to the degree of constriction considered. In contrast, complete blockage produces great reductions in deposition, which intensify with penetration into the lungs and are prominent in the pulmonary compartment.

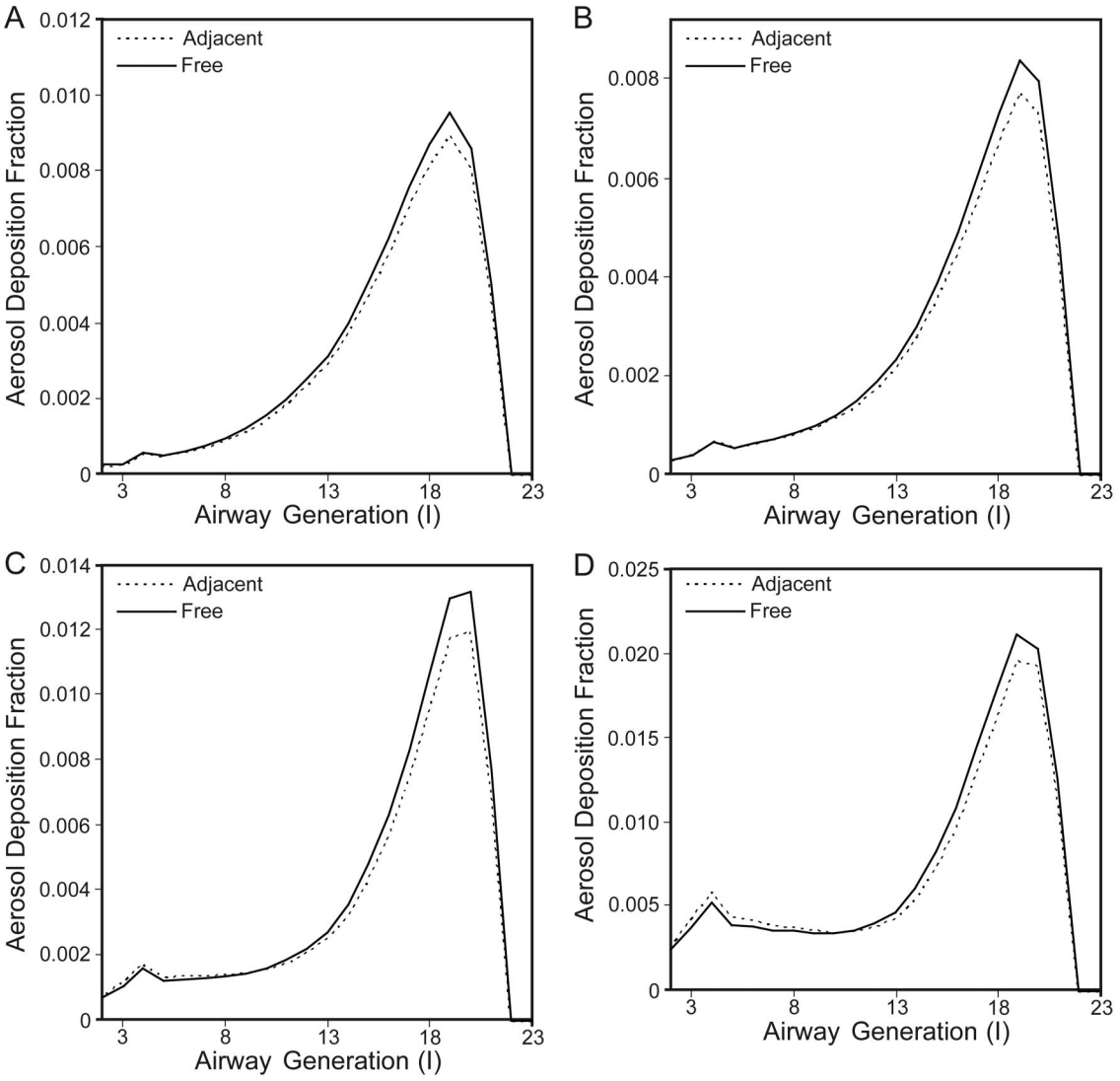

Fig. 12. Aerosol deposition patterns for sedentary respiratory activity along identified branch morphologies for severe respiratory disease (complete blockage). Particle sizes are 0.5 μm (panel A), 1.0 μm (panel B), 2.0 μm (panel C), and 4.0 μm (panel D) diameter.

Figures 10 to 13 illustrate aerosol deposition patterns along identified branching morphologies. Therefore, they address the seminal question: within lungs, how does the physical manifestation of disease affect aerosol deposition from the site of disease (ie, generation I = 2 in our case) to the alveolar sacs positioned at I = 23? The resulting observations may be of clinical importance when treating patients with diseases preferentially located in either the upper or lower airways throughout the lungs. This is the case simply because by affecting air flow patterns, airway constrictions and blockages affect the transport and thus ultimately the deposition of inhaled pharmacologic drugs. For example, constricted airways may become sites of enhanced deposition due to increased effectiveness of the inertial impaction deposition mechanism[21] and may influence the delivery of aerosols to downstream regions.

Considering Figures 10 to 13, we note that for the 50% constriction there is a marked decrease in deposition in the upper airways and a significant increase more distally, especially in the pulmonary region. These observations can be attributed to the fact the flow through the constricted branch is reduced by about 40%, as can be inferred from Figure 2, and to the effects this change in flow will have on the deposition mechanisms alluded to in the Introduction. That is, the decreased deposition may be observed within the airways downstream of the constriction due to the decrease in the efficiency of the inertial impaction deposition mechanism. This same reduced velocity

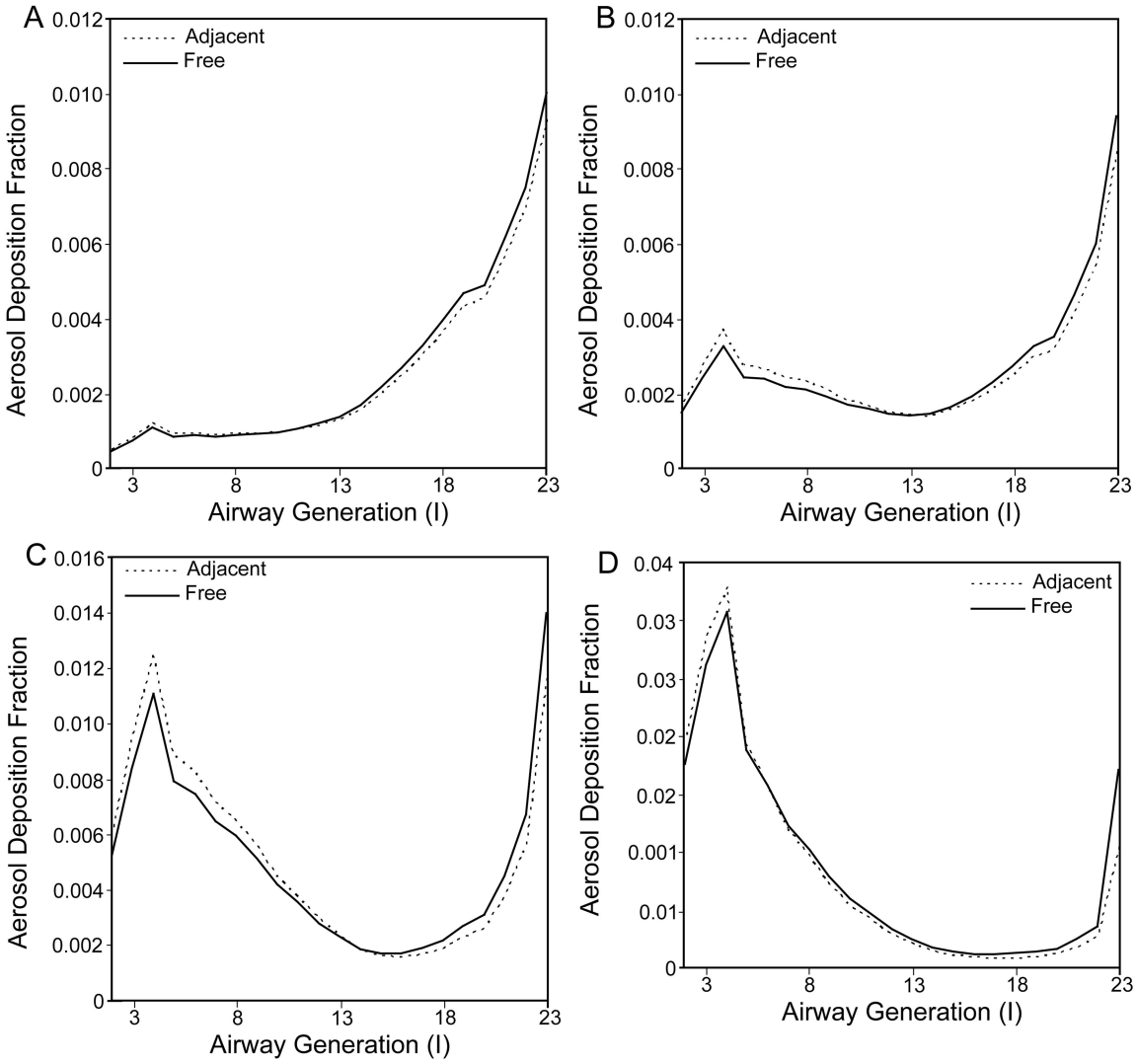

Fig. 13. Aerosol deposition patterns for pronounced respiratory activity along identified branch morphologies for severe respiratory disease (complete blockage). Particle sizes are 0.5 μm (panel A), 1.0 μm (panel B), 2.0 μm (panel C), and 4.0 μm (panel D) diameter.

results in an increase in deposition deeper in the lung, where the mechanisms of sedimentation and diffusion are dominant. On the other hand, the adjacent and free branches exhibit relatively little difference in deposition, because there is a much smaller difference in flow between them.

There is little difference in deposition between the adjacent and free branches for a given breathing condition. However, there are major differences between different respiratory regimes.

In summary, we have presented a series of illustrations documenting the key parameters affecting inhaled drug delivery and their strong inter-relations. Our results demonstrate that respiratory diseases, by affecting airway morphologies and ventilation (redistribution of air flow) will influence the deposition of inhaled drugs used in their treatment.

Conclusions

Using a validated aerosol dosimetry model coupled with a flow distribution model, we have described the results of a systematic and comprehensive computational study of particle deposition patterns within healthy and diseased lungs. Pathologies were simulated by constrictions and blockages, which caused uneven flow distributions. We considered a range of respiratory intensities, from sedentary to pronounced states, and calculated the deposition patterns of particle sizes ranging from 0.1 μm to 10 μm. Because of the complexities involved when interpreting interactive effects between diseased airway morphologies and redistributed air flows on the transport and deposition of inhaled particles, drug delivery to diseased lungs should be considered on a case-by-case basis. Mathematical mod-

eling should be used as a complementary tool for performing predictive simulations, analyzing the results, and therefore customizing the aerosol therapy protocols to patients. We suggest that this sound scientific approach may get inhaled pharmaceuticals targeted to appropriate sites to elicit positive therapeutic effects and decrease adverse effects.

ACKNOWLEDGMENTS

For assistance on this project, we thank Ing Chea Ang and Christopher Harty, who were affiliated with the Department of Mechanical Engineering, Lafayette College, Easton, Pennsylvania, at the time of this research.

REFERENCES

1. Usmani OS, Biddiscombe MF, Barnes PJ. Regional lung deposition and bronchodilator response as a function of β_2-agonist particle size. Am J Respir Crit Care Med 2005;172(12):1497-1504.
2. Cryan SA. Carrier-based strategies for targeting protein and peptide drugs to the lungs. AAPS J 2005;7(1):E20-E41.
3. Witek TJ. The fate of inhaled drugs: the pharmacokinetics and pharmacodynamics of drugs administered by aerosol. Respir Care 2000; 45(7):826-830.
4. Laube B. The expanding role of aerosols in systemic drug delivery, gene therapy, and vaccination. Respir Care 2005;50(9):1161-1174.
5. Verbanck S, Schuermans D, Paiva M, Vincken W. The functional benefit of anti-inflammatory aerosols in the lung periphery. J Allergy Clin Immunol 2006;118(2):340-346.
6. Smaldone GC, Dickinson, Marcial GE, Young E, Seymour J. Deposition of aerosolized pentamidine and failure of pneumocystis prophylaxis. Chest 1992;101(1):82-87.
7. Kim CS, Brown LK, Lewars CG, Sackner MA. Deposition of aerosol particles and flow resistance in mathematical and experimental airways. Appl Physiol Respir Environ Exercise Physiol 1983;55: 154-163.
8. Martonen TB. Aerosol therapy implications of particle deposition patterns in simulated human airways. J Aerosol Med 1991;4(1):25-40.
9. Zeidler MR, Kleerup EC, Goldin JG, Kim HJ, Truong DA, Simmons MD, et al. Montelukast improves regional air-trapping due to small airways obstruction in asthma. Eur Respir J 2006;27(2):307-315.
10. Martonen TB, Katz IM, Cress W. Aerosol deposition as a function of airway disease: cystic fibrosis. Pharm Res 1995;12(1):96-102.
11. Kim CS, Fisher DM, Lutz DJ, Gerrity TR. Particle deposition in bifurcating airway models with varying airway geometry. J Aerosol Sci 1994;25(3):567-581.
12. Asgharian B, Price OT, Hofmann W. Prediction of particle deposition in the human lung using realistic models of lung ventilation. J Aerosol Sci 2006;37:1209-1221.
13. Pedley TJ, Schroter RC, Sudlow MF. The prediction of pressure drop and variation of resistance within the human bronchial airways. Respir Physiol 1970;9:387-405.
14. Martonen TB, Rosati JA, Isaacs KK. Modeling deposition of inhaled particles. In: Ruzer LS, Harley NH, editors. Aerosols handbook: measurement, dosimetry and health effects. New York: CRC Press; 2005:113-155.
15. Martonen TB. Mathematical model for the selective deposition of inhaled pharmaceuticals. J Pharm Sci 1993;82(12):1191-1199.
16. Martonen TB, Musante CJ, Segal RA, Schroeter JD, Hwang D, Dolovich M, et al. Lung models: strengths and limitations. Respir Care 2000;45(6):712-736.
17. Segal RA, Martonen TB, Kim CS, Shearer M. Computer simulations of particle deposition in the lungs of chronic obstructive pulmonary disease patients. Inhal Toxicol 2002;14(7):101-116.
18. Martonen TB, Fleming JS, Schroeter JD, Conway J, Hwang D. In silico modeling of asthma. Adv Drug Del Rev 2003;55(7):829-849.
19. Martonen TB, Isaacs KK, Hwang D. Three-dimensional simulations of airways within human lungs. Cell Biochem Biophys 2005;42(3): 223-249.
20. Martonen TB, Smyth H, Isaacs K, Burton R. Issues in drug delivery: concepts and practice. Respir Care 2005;50(9):1228-1252.
21. Isaacs KK, Rosati JA, Martonen TB. Mechanisms of particle deposition. In: Ruzer LS, Harley NH, editors. Aerosols handbook: measurement, dosimetry and health effects. New York: CRC Press;2005: 75-99.
22. Soong TT, Nicolaides P, Yu CP, Soong SC. A statistical description of the human tracheobronchial tree geometry. Respir Physiol 1979; 37:161-172.
23. Weibel ER. Morphometry of the human lung. Berlin: Springer-Verlag; 1963.